Optics Letters

Detection and perfect fitting of 13.2 dB squeezed vacuum states by considering green-light-induced infrared absorption

Shaoping Shi,[1,2] Yajun Wang,[1,2] Wenhai Yang,[1,2] Yaohui Zheng,[1,2,*] and Kunchi Peng[1,2]

[1]*The State Key Laboratory of Quantum Optics and Quantum Optics Devices, Institute of Opto-Electronics, Shanxi University, Taiyuan 030006, China*
[2]*Collaborative Innovation Center of Extreme Optics, Shanxi University, Taiyuan, Shanxi 030006, China*
Corresponding author: yhzheng@sxu.edu.cn

We report on a high-level squeezed vacuum state with maximum quantum noise reduction of 13.2 dB directly detected at the pump power of 180 mW. The pump power dependence of the squeezing factor is experimentally exhibited. When considering only loss and phase fluctuation, the fitting results have a large deviation from the measurement value near the threshold. By integrating green-light-induced infrared absorption (GLIIRA) loss, the squeezing factor can be perfectly fitted in the whole pump power range. The result indicates that GLIIRA loss should be thoroughly considered and quantified in the generation of high-level squeezed states. © 2018 Optical Society of America

Squeezed states, which have fewer fluctuations in one quadrature than vacuum noise at the expense of increased fluctuations in the other quadrature [1], can be used to enhance measurement precision [2–6], increase detection sensitivity [7–9], and improve fault tolerance performance for quantum information and quantum computation [10]. All of these performance improvements strongly depend on the squeezing level of squeezed states. The optical parametric process has been proven to be the most successful system for squeezed state generation [11–16], especially for the generation of high-level squeezed states.

Although the first experimental demonstration of squeezed states based on the optical parametric oscillator (OPO) succeeded in 1986 [17], in the following two decades, dedicated research could achieve only typical squeezing factors of 3 dB to 6 dB [18–20]. In 2007, researchers at the University of Tokyo took a giant step forward and obtained a factor of 9 dB quantum noise reduction at 860 nm [16]. Under the motivation of gravitational waves detection, a 10 dB squeezed vacuum state was detected for the first time at the University of Hanover in 2007 [11]. Subsequently, the squeezing strength was gradually increased [12,13], reaching the maximum value of 15 dB at l064 nm based on periodically poled KTiOPO$_4$ (PPKTP) [14]. In ideal conditions, an infinite squeezing factor can be

generated and detected at the threshold. However the non-ideal components introduce inevitable loss during generation, propagation, and detection of squeezed states. This loss reduces the squeezing factor by introducing vacuum noise into the squeezed state, finally limiting the squeezing factor [14,21,22]. The closer the OPO operates to its oscillation threshold, the stronger the squeezing factor is. Phase fluctuation is another limiting factor of the squeezing level by coupling the anti-squeezing quadrature into the squeezed quadrature in the measurement [16,20,22–25]. An increase of the pump power also increases the generated amount of anti-squeezing factor, which aggravates the influence of the anti-squeezed quadrature on the measured squeezing factor with a phase fluctuation. Therefore, there exists an optimal pump factor, dependent on the phase fluctuation, at which the measured squeezing factor is maximum. The optimal value gradually approaches the oscillation threshold of the OPO with improvement of the phase fluctuation. For scaling the squeezing factor to a new height, current researches focus mainly on the reduction of loss and phase fluctuation [14,16,22]. After those key optimizations, the construction of a photodetector with low noise, high gain, and high common-mode-rejection ratio becomes a major measurement accuracy limitation for reducing electronic noise from the photodetector, and classical noise from the local oscillator [26–29].

For squeezed state generation at 1064 nm, a 532 nm harmonic beam is poured into the OPO as a pump light. The illumination of PPKTP with 532 nm lasing also induces an intensity-dependent absorption of its down-conversion beam. It is referred to as green-light-induced infrared absorption (GLIIRA) [30,31], which increases loss and deteriorates squeezing strength. At a low squeezed level, the squeezing factor is insensitive to optical and detection losses, in which the GLIIRA loss can be ignored [16,32,33]. The loss dependence becomes acute as the squeezing factor increases. In addition, the amount of squeezing generated has only a square-root dependence on the pump power [22,34]; the increase of pump power for a high squeezing factor induces higher GLIIRA loss in comparison with the status of a low squeezing factor. In order to detect a high-level squeezed state, it becomes urgent to consider

and quantify the influence of GLIIRA loss on the squeezing factor in terms of an actual crystal sample.

In this Letter, we report a high-level squeezed vacuum state with a maximum quantum noise reduction of 13.2 dB directly detected at the pump power of 180 mW. Considering the contribution of electronic noise, the maximum squeezing level is up to 13.35 dB. The squeezing and anti-squeezing factors are repeatedly measured at several pump powers. According to measurement results, the pump power dependence of the squeezing factor can be fitted by using the expression of squeezed and anti-squeezed quadrature variances. When only considering loss and phase fluctuation, the fitting result deviates from measurement data in the near-threshold section. By integrating GLIIRA loss, the squeezing factor can be perfectly fitted in the pump power range from 0 to the threshold. The result indicates that the GLIIRA loss should be thoroughly considered and quantified in the generation of a high-level squeezed state.

A schematic of our experimental setup is shown in Fig. 1. The laser source is a single-frequency Nd:YVO$_4$ laser at 1064 nm. The laser transmits through a mode cleaner for spatial-temporal filtering and polarization purifying of the downstream experiment. Approximately 100 mW of the transmitted light is reserved as an auxiliary beam for mode matching between the downconversion beam and the OPO, measurement of the classical parametric gain, the adjustment of the interference efficiency between the downconversion beam and local oscillator. A fraction of the transmitted light (30 mW) serves as the local oscillator. The remaining light is used for second-harmonic generation (SHG) to provide a 532 nm pump field of the OPO. Another two mode cleaners are positioned in the optical paths of the local oscillator and pump beam, to serve as optical low-pass filters as well as spatial mode cleaners. These mode cleaners are held on resonance with the laser wavelength via a Pound–Drever–Hall technique [35]. By using an auxiliary cavity adjustment technique [36,37], all of the mode-matching efficiencies in the downstream experiment are significantly improved and reach optimal performance. Fringe visibility between the squeezed beam and local oscillator reaches 99.8%. Both the downconversion and pump beams have mode-matching efficiency of more than 99.8% with the OPO. High-efficiency

mode matching is advantageous not only to enhancement of the squeezing factor, but also reduction of the GLIIRA loss.

Our OPO is a semi-monolithic cavity consisting of a piezoactuated concave mirror and a PPKTP crystal with dimensions of 10 mm × 2 mm × 1 mm and refractive index of 1.83. The crystal end face with a curvature radius of 12 mm is coated as high reflectivity (HR) for the fundamental beam and high transmission for the pump beam, thus serving as one of the cavity mirrors. The plane face of the crystal is coated as anti-reflectivity (AR) for both wavelengths. The intracavity loss, comprising the residual transmission through the HR-coated end facet, the residual reflection of AR-coated end facet, is 0.2 ± 0.05%. The crystal temperature is stabilized at 35.6°C to obtain the optimal phase-matching condition. An air gap of 25.1 mm length is realized between the AR-coated side of the crystal and the coupling mirror, and formed a 33 μm waist radius at the fundamental wave. The concave mirror with a radius of curvature of 30 mm has a transmissivity of 12 ± 0.5% for 1064 nm and HR for 532 nm, which is used as the output coupler. Without the pump beam illuminating, the escape efficiency is inferred as $\eta_{esc} = 98.34 \pm 0.47\%$.

The squeezed light emitted from the concave mirror is separated from the pump light by a dichroic beam splitter, and carefully mode matched with the local oscillator on a 50/50 beam splitter. The output beam from the 50/50 beam splitter is directed toward a balanced homodyne detection (BHD) to observe noise level. The BHD, with the common mode rejection ratio of 75 dB [29], is built from a pair of p-i-n photodiodes (from Laser Components) with a quantum efficiency more than 99%. To recycle the residual reflection from photodiode surfaces, two concave mirrors with a curvature radius of 50 mm are used as retroreflectors.

GLIIRA loss is measured by comparing mode-matching efficiency of an optical cavity with and without 532 nm laser illuminating, which has a measurement sensitivity better than 10^{-5}/cm [38,39]. We perform the measurement of GLIIRA at the pump power from 50 mW to 230 mW with a step of 15 mW, corresponding to the power density from 2.9 kW/cm^2 to 13.34 kW/cm^2 in PPKTP, and the GLIIRA absorption coefficient from 1.21×10^{-4}/cm to 1.12×10^{-3}/cm. According to measurement results of the actual used power level, the GLIIRA coefficient can be fitted with the expression of $\alpha_{GLIIRA} = 6.23 \times 10^{-6} \times I_g^2 + 2.32 \times 10^{-5} \times I_g$ (I_g is the power density at 532 nm light with the unit of kW/cm^2). With this result, we can infer that GLIIRA loss would reduce the squeezing level by 0.04 dB for a squeezing factor of 9 dB, which can be neglected, while the decrease is 1.17 dB for 15 dB squeezing.

Figure 2 presents the measured results of a squeezed vacuum state at the pump power of 180 mW. All traces are measured by a spectrum analyzer (Agilent N9020A with the uncertainty of 0.2 dB). Trace (a) corresponds to the shot noise of 5.5 mW local oscillator power and is measured with the squeezed light blocked. Trace (b) shows the quantum noise reduction when squeezed states are injected with the local oscillator phase scanned. The directly observed squeezing level is 13.2 dB at the analysis frequency of 3 MHz without subtracting electronic noise. The corresponding anti-squeezing is 24.7 dB above the shot noise limit (SNL). Trace (c) is electronic noise, which is 28 dB below the SNL at the local oscillator power of 5.5 mW.
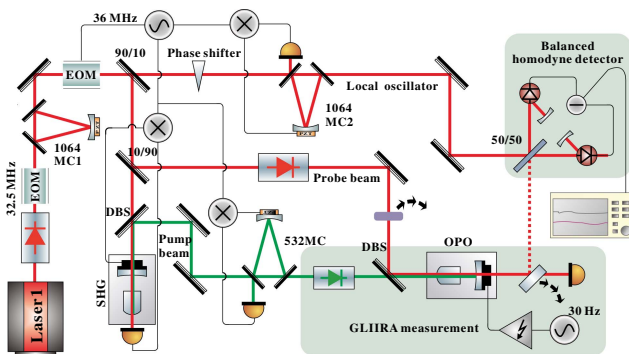

Fig. 1. Schematic of the experimental setup for the squeezed state generation and GLIIRA measurement. SHG, second-harmonic generation; EOM, electro-optical modulator; MC, mode cleaner; OPO, optical parametric oscillator; DBS, dichroic beam splitter; PBS, polarization beam splitter; HWP, half-wave plate; GLIIRA, green-light-induced infrared absorption.
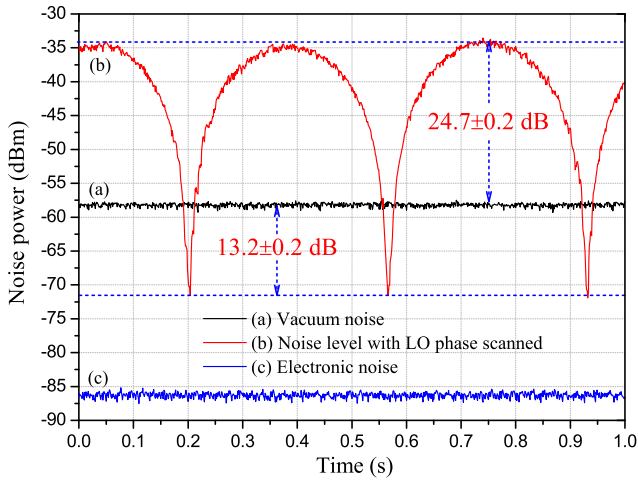
Fig. 2. Balanced homodyne measurements of the quadrature noise variances. The measurement is recorded at a fourier frequency of 3 MHz, with a RBW of 300 kHz, and a VBW of 200 Hz. The data still include electronic noise.

We also observe the power-dependent squeezing and anti-squeezing. During the measurement, the OPO is kept on resonance by manually applying offset voltage to the piezo, which is attached to the output mirror of the OPO. The results are shown in Fig. 3 with black squares. All measurement data are normalized to the vacuum noise. Here, the contribution of electronic noise is corrected, and hence the optimum squeezing factor can reach up to 13.35 dB. Due to a 99.8% mode-matching efficiency between the pump beam and the OPO, the pump power is not corrected. The absolute error of a given pump power is 3% on account of the measurement uncertainty of the power meter. More than 20 times squeezing and anti-squeezing factors are measured at each power level, then the standard deviations are calculated as the vertical error bars.

The squeezed and anti-squeezed quadrature variances for our OPO can be modeled by [34]
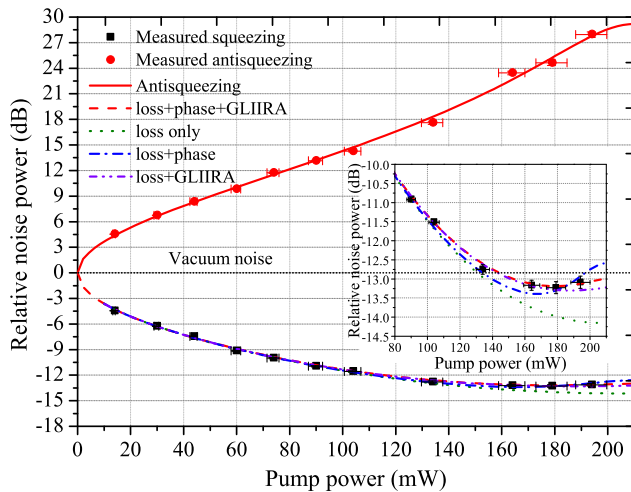

Fig. 3. Pump power dependence of anti-squeezed and squeezed quadrature variances. All the data are dark-noise corrected and normalized to the vacuum reference.

$$V_{s/a} = \left[1 \mp \eta_{\text{tot}} \frac{4\sqrt{P/P_{\text{th}}}}{\left(1 \pm \sqrt{P/P_{\text{th}}}\right)^2 + 4\kappa^2} \right] \cos^2 \theta$$

$$+ \left[1 \pm \eta_{\text{tot}} \frac{4\sqrt{P/P_{\text{th}}}}{\left(1 \mp \sqrt{P/P_{\text{th}}}\right)^2 + 4\kappa^2} \right] \sin^2 \theta, \quad (1)$$

where P is the pump power, P_{th} is the threshold power, and θ is the phase fluctuation. $\eta_{\text{tot}} = \eta_{\text{esc}}\eta_{\text{pro}}\eta_{\text{vis}}\eta_{\text{qe}}$ is the total loss of the squeezing generation, propagation, and detection, $\eta_{\text{esc}} = T/(T + L + \alpha_{\text{GLIIRA}})$ is the escape efficiency, η_{pro} is the propagation efficiency, η_{vis} is the square of the homodyne visibility, and η_{qe} is the quantum efficiency of the photo diodes. $\kappa = 2\pi f/\gamma$ is the dimensionless parameter, f is the Fourier frequency, and $\gamma = c(T + L + \alpha_{\text{GLIIRA}})/2l$ is the decay rate. T is the transmissivity of the output coupler, α_{GLIIRA} is the GLIIRA coefficient, c is the vacuum speed of light, L is the total intracavity linear loss of the OPO, and l is the single-trip length of the OPO.

Here, $l = 35.1$ mm, $f = 3$ MHz, OPO linewidth $\nu = 71.5$ MHz, propagation efficiency $\eta_{\text{pro}} = 99.4\%$, and threshold power $P_{\text{th}} = 210$ mW. Total loss of the squeezed state generation system can be inferred between 2.2% and 4.1%. According to the known parameters in our experimental system, the difference in the squeezing factor is only 0.08 dB at worst with and without GLIIRA and phase fluctuation (4.5 mrad) at the pump power of less than 75 mW, which can be neglected. Therefore, total loss of the squeezed state generation system can be obtained by fitting the pump power dependence of the squeezing factor in the range of 0 mW and 75 mW. The fitting result is $3.73 \pm 0.15\%$ within range of our inference. Since the projection of the squeezing quadrature can be neglected, the discrepancy of the anti-squeezing factor is very small with and without GLIIRA and phase fluctuation. By independently fitting the pump power dependence of the anti-squeezing factor, we obtain that total loss is $3.7 \pm 0.05\%$, which is in agreement with the fitting of the squeezing factor. This further confirms that total loss from the fitting is credible. According to the known loss, the power dependence of the squeezing factor is calculated without considering GLIIRA and phase fluctuation, shown in the dotted line in Fig. 3. Discrepancy between the calculated and measured values becomes obvious as the pump power increases.

The influence of GLIIRA and phase noise on the squeezing factor becomes more remarkable as the pump power is increased, due to the quadratic increase of the GLIIRA factor and rapid growth of the anti-squeezing factor. Therefore, the squeezing factor cannot be solely determined by the total loss at higher pump power. Actually, the intracavity loss is not a constant with the pump beam illuminating. As a result, escape efficiency η_{esc} decreases with an increase of the pump power. In the pump power range from 0 to the threshold power, the variation of the threshold power, originating from GLIIRA loss, can be neglected. Following the total loss obtained above, we can fit the pump power dependence of squeezing with known loss and unknown phase fluctuation, shown in the dashed-dotted line in Fig. 3, corresponding to a fitting phase fluctuation of 4.42 ± 0.22 mrad. However, the fitting values are more than the measured ones at less than the power point where the squeezing factor is optimal, and vice verse. Maximum deviation is about 0.5 dB. Supposing the phase fluctuation is zero, we can

calculate the power dependence of the squeezing factor on the basis of known loss and GLIIRA factor, shown in the dashed-dotted dot line in Fig. 3. Comparing with only the loss, the deviation is reduced, especially in the pump power range from 90 mW to 165 mW. However, it is always more than the measurement value near the threshold; the discrepancy tends to increase with pump power. The result indicates that the phase fluctuation relative to GLIIRA is the main dependent element of the squeezing factor.

On the basis of known loss and GLIIRA expression, we can fit the pump power dependence of squeezing factors, shown in the dashed line in Fig. 3, corresponding to a fitting phase fluctuation of 1.76 ± 0.52 mrad. The fitting result is in good agreement with the experimental results in the whole pump power range. All of these fitting procedures are on the basis of the mean value of measured data by using the simplex method within the Origin software; no standard deviation is considered. Therefore, the experimental results confirm that GLIIRA loss should be quantified and analyzed to optimize the squeezing factor for the generation of a high-level squeezed state. Especially for the periodically poled crystal, the poled process provides more possibilities for color centers to be formed in the material, which brings in a higher amplitude of GLIIRA than the birefringence phase-matching one [30]. Meanwhile, GLIIRA loss depends strongly on the crystalline growth and polarization conditions, which should be solely considered from sample to sample. It is worth noting that pump power dependence of the squeezing factor presents an inflection point at which the squeezed degree is optimal. The optimal squeezed degree depends on crystal length, OPO parameters, crystalline quality, pump power, and GLIIRA loss. This spurs us to optimize systematically these experimental parameters according to the actual crystal sample to achieve the best squeezing factor.

In conclusion, we report on a high-level squeezed vacuum state with maximum quantum noise reduction of 13.2 dB directly detected at the pump power of 180 mW. After correcting the contribution of electronic noise, the optimum squeezing factor reaches 13.35 dB. We repeat the squeezing and anti-squeezing measurement for several pump powers, and obtain pump power dependence of the squeezing and anti-squeezing factors. Measurement results cannot be completely fitted in the whole power range when considering only the loss and phase fluctuation. In combination with the measurement results of GLIIRA loss, we can perfectly fit the pump power dependence of the squeezing factor. The result indicates that GLIIRA loss should be thoroughly considered and quantified in the generation of high-level squeezed states.

REFERENCES

1. D. F. Walls, Nature **306**, 141 (1983).
2. R. Schnabel, N. Mavalvala, D. E. McClelland, and P. K. Lam, Nat. Commun. **1**, 121 (2010).
3. S. Steinlechner, J. Bauchrowitz, M. Meinders, H. Muellerebhardt, and K. Danzmann, Nat. Photonics **7**, 626 (2013).
4. M. Xiao, L. A. Wu, and H. J. Kimble, Phys. Rev. Lett. **59**, 278 (1987).
5. J. Kong, Z. Y. Ou, and W. P. Zhang, Phys. Rev. A **87**, 023825 (2013).
6. Z. Y. Ou, Phys. Rev. A **85**, 023815 (2012).
7. Y. Q. Li, D. Guzun, and M. Xiao, Phys. Rev. Lett. **82**, 5225 (1999).
8. C. L. Degen, F. Reinhard, and P. Cappellaro, Rev. Mod. Phys. **89**, 035002 (2017).
9. U. L. Andersen, T. Gehring, C. Marquardt, and G. Leuchs, Phys. Scr. **91**, 053001 (2016).
10. N. C. Menicucci, Phys. Rev. Lett. **112**, 120504 (2014).
11. H. Vahlbruch, M. Mehmet, S. Chelkowski, B. Hage, A. Franzen, N. Lastzka, S. Goßler, K. Danzmann, and R. Schnabel, Phys. Rev. Lett. **100**, 033602 (2008).
12. M. Mehmet, S. Ast, T. Eberle, S. Steinlechner, H. Vahlbruch, and R. Schnabel, Opt. Express **19**, 25763 (2011).
13. T. Eberle, S. Steinlechner, J. Bauchrowitz, V. Händchen, H. Vahlbruch, M. Mehmet, H. Müller-Ebhardt, and R. Schnabel, Phys. Rev. Lett. **104**, 251102 (2010).
14. H. Vahlbruch, M. Mehmet, K. Danzmann, and R. Schnabel, Phys. Rev. Lett. **117**, 110801 (2016).
15. T. Serikawa, J. Yoshikawa, K. Makino, and A. Frusawa, Opt. Express **24**, 28383 (2016).
16. Y. Takeno, M. Yukawa, H. Yonezawa, and A. Furusawa, Opt. Express **15**, 4321 (2007).
17. L. Wu, H. J. Kimble, J. L. Hall, and H. Wu, Phys. Rev. Lett. **57**, 2520 (1986).
18. N. Treps, N. Grosse, W. P. Bowen, C. Fabre, H. A. Bachor, and P. K. Lam, Science **301**, 940 (2003).
19. T. C. Zhang, K. W. Goh, C. W. Chou, P. Lodahl, and H. J. Kimble, Phys. Rev. A **67**, 033802 (2003).
20. Y. Wang, H. Shen, X. J. Jia, X. L. Su, C. D. Xie, and K. C. Peng, Opt. Express **18**, 6149 (2010).
21. P. K. Lam, T. C. Ralph, B. C. Buchler, D. E. McClelland, H. A. Bachor, and J. Gao, J. Opt. B **1**, 469 (1999).
22. S. Dwyer, L. Barsotti, S. S. Y. Chua, M. Evans, M. Factourovich, D. Gustafson, T. Isogai, K. Kawabe, A. Khalaidovski, P. K. Lam, M. Landry, N. Mavalvala, D. E. McClelland, G. D. Meadors, C. M. Mow-Lowry, R. Schnabel, R. M. S. Schofield, N. Smith-Lefebvre, M. Stefszky, C. Vorvick, and D. Sigg, Opt. Express **21**, 19047 (2013).
23. E. Oelker, G. Mansell, M. Tse, J. Miller, F. Matichard, L. Barsotti, P. Fritschel, D. E. McClelland, M. Evans, and N. Mavalvala, Optica **3**, 682 (2016).
24. K. Schneider, M. Lang, J. Mlynek, and S. Schiller, Opt. Express **2**, 59 (1998).
25. E. Oelker, L. Barsotti, S. Dwyer, D. Sigg, and N. Mavalvala, Opt. Express **22**, 21106 (2014).
26. H. J. Zhou, W. H. Yang, Z. X. Li, X. F. Li, and Y. H. Zheng, Rev. Sci. Instrum. **85**, 013111 (2014).
27. H. J. Zhou, W. Z. Wang, C. Y. Chen, and Y. H. Zheng, IEEE Sens. J. **15**, 2101 (2015).
28. M. S. Stefszky, C. M. Mow-Lowry, S. S. Y. Chua, D. A. Shaddock, B. C. Buchler, H. Vahlbruch, A. Khalaidobski, R. Schnabel, P. K. Lam, and D. E. McClelland, Classical Quantum Gravity **29**, 145015 (2012).
29. X. L. Jin, J. Su, Y. H. Zheng, C. Y. Chen, W. Z. Wang, and K. C. Peng, Opt. Express **23**, 23859 (2015).
30. S. Wang, V. Pasiskevicius, and F. Laurell, J. Appl. Phys. **96**, 2023 (2004).
31. M. Roth, N. Angert, M. Tseitlin, and A. Alexandrovski, Opt. Mater. **16**, 131 (2001).
32. S. Suzuki, H. Yonezawa, F. Kannari, M. Sasaki, and A. Furusawa, Appl. Phys. Lett. **89**, 061116 (2006).
33. M. Stefszky, C. M. Mow-Lowry, K. McKenzie, S. Chua, B. C. Buchler, T. Symul, D. E. McClelland, and P. K. Lam, J. Phys. B **44**, 015502 (2011).
34. W. H. Yang, S. P. Shi, Y. J. Wang, W. G. Ma, Y. H. Zheng, and K. C. Peng, Opt. Lett. **42**, 4553 (2017).
35. E. D. Black, Am. J. Phys. **69**, 79 (2001).
36. Y. J. Lu and Z. Y. Ou, Phys. Rev. A **62**, 033804 (2000).
37. M. Mehmet, H. Vahlbruch, N. Lastzka, K. Danzmann, and R. Schnabel, Phys. Rev. A **81**, 013814 (2010).
38. Y. J. Wang, W. H. Yang, Z. X. Li, and Y. H. Zheng, Sci. Rep. **7**, 41405 (2017).
39. Y. J. Wang, Z. X. Li, Y. H. Zheng, and J. Su, IEEE J. Quantum Electron. **53**, 7000307 (2017).